In: 2023 AIAA Aviation and Aeronautics Forum and Exposition (AIAA AVIATION Forum), 12-16 June 2023, San Diego, CA
DOI: 10.2514/6.2023-3867

Fusion Insights from Ultrasonic and Thermographic Inspections for Impact Damage Analysis

Muhammet E. Torbali*, Muflih Alhammad †, Argyrios Zolotas ‡, Nicolas P. Avdelidis §
Cranfield University, Bedford, UK, MK43 0AL

Clemente Ibarra-Castanedo¶, Xavier P. Maldague‖
Universite Laval, Quebec, Canada, G1V 0A6

Low energy impact damage in composite materials may be more concerning than it appears visually, often requiring a detailed examination for accurate assessment to ensure safe and sustainable operation. Non-destructive testing (NDT) methods provide such inspection techniques, and in this paper, NDT-based fusion is explored for enhanced identification of defect size and location compared to indepdently using individual NDT methods separately. Three Carbon Fiber Reinforced Polymer (CFRP) specimens are examined, each with an impact damage of a given energy level, using pulsed thermography (PT) and phased array (PA) ultrasonic methods. Following the extraction of binary defect shapes from source images, a decision-level fusion approach is performed. The results indicate that combining ultrasonic and infrared thermography (IRT) inspections for CFRP composite materials is promising to achieve enhanced and improved detection traceability.

I. Nomenclature

$CFRP$	=	Carbon Fibre Reinforced Polimers
IRT	=	Infrared Thermography
KJ	=	Kilojoules
MRO	=	Maintenance Repair Operations
NDT	=	Non-destructive Testing
UT	=	Ultrasonic Testing
PA	=	Phased Array
PCA	=	Principle Component Analysis
PT	=	Pulsed Thermography
SNR	=	Signal-to Noise Ratio

II. Introduction

Composite structures form a popular material utilised in many fields, from space applications to civil engineering, due to their lightweight per unit material and improved axial robustness properties [1]. The aviation industry looks at composite materials favourably as they provide structural strength yet with lighter weight. Regardless of the structures and materials used, a safe and sustainable operation is of paramount importance, which necessitates efficient Maintenance, Repair, Operations (MRO). Referring to aviation, air vehicles and their components need to be checked at certain times or under a cyclic period to assess functionality. Detailed maintenance stage may take considerable time, which may have serious consequences such as vehicles being grounded for longer periods and hence also having a negative impact on operations. Non-destructive testing (NDT) enables efficient and timely inspections (maintaining the

*Student, Aerospace Department,MK43 0AL.
†Student, Aerospace Department,MK43 0AL.
‡Reader, Aerospace Department, MK43 0AL.
§Professor, Aerospace Department, MK43 0AL.
¶Research professional, Department of Electrical and Computer Engineering, G1V 0A6.
‖Professor, Department of Electrical and Computer Engineering, G1V 0A6.

standard with reduced maintenance costs) [2, 3]; hence they can play an important role in industries like the aviation industry.

There is a variety of NDT methods [4], and among these, ultrasonic testing (UT) techniques are commonly used in aircraft structures inspection [5]. In particular, the Ultrasonic phased array, due to its multiple ultrasonic element nature, can provide efficient scans even statically (depending on the requirements of the inspection). These ultrasonic elements emit waves into the material that are reflected back to the probe. A non-defective material would be seen by an intact reflected signal, while in the case of defects, the signal is scattered and subject to attenuation levels. Ultrasonic PA can be used to inspect large areas efficiently given its phased-array setup, however, it suffers from providing appropriate near-surface detection due to the blind zone effect, which hinders defect detection due to the aftershocks near the probe [6].

Another NDT method is infrared thermography (IRT), which is a condition monitoring technique that, from a measurement of the radiant heat pattern emitted by a material, is able to determine regions or points of increased or reduced heat emission that can indicate the presence of an imperfection in the investigated material and seems appealing in terms of accuracy and spatial precision provided [7]. Different to UT, IRT suffers from inspecting thick structures (deeper sub-surface defects); because it uses infrared technology, it cannot penetrate in extended depths (only a few millimetres) [8].

Individual NDT approaches tend to offer distinct information about material conditions, albeit merging information of diverse NDT methods may yield greater insights. Data fusion is well-known for combining (fusing) data from various sensors (sources), in the context of NDT inspection data information from different inspection technologies. Several works in NDT fusion have already appeared in the literature that focus on various material types such as concrete [9], metallic [10], or composite [11] structures. Although not without challenges in its application, data fusion can potentially be used to enhance defect detection and characterization through advanced fusion operations. In this study an improved solution for localizing and sizing low-energy impact defects, by combining infrared thermography (IRT) and ultrasonic phased array (UT PA) inspection methods, is proposed.

III. Material and Methods

A. Sample description

A set of CFRP composite laminates formed by 18 plies, 3.8 mm thickness and 100x150 mm size have been used (representing composite material in aerospace structures). The coupons were made from UD pre-preg IMS-977-2 material with $[45/-45/90/0/90/0/90/-45/45]_{2s}$ layup commonly found in aviation composites. Samples have been impacted under ASTM standards with three different energy levels (8J, 12J and 20J) to compare the visibility of different-sized defects. Figure 1 shows an example of composite coupons from both sides to observe thickness and dimensions. Both surfaces seem sound and smooth, meaning there is no visible damage on the surfaces.

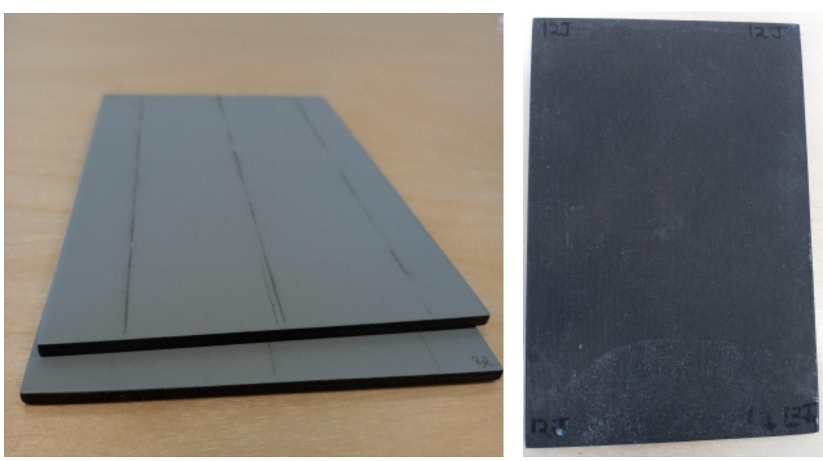

(a) Composite coupons with 3.8mm thickness (b) Back side of 12 J defected sample

Fig. 1 Image of composite samples that exhibit no surface defect

B. Pulsed thermography inspection

The thermal inspection was performed by pulsed thermography, and samples were subjected to two 6.2 kJ output energy heat sources, Xenon arc flashes, for a duration of 2 ms, from a 50 cm distance and 45° angles to the surface of the samples. Thermal images have been recorded by X6900 FLIR infrared camera, from 100 cm distance and 90° angles to the sample surface, with an InSb-CCD Matrix Sensor and image resolution of 640 × 512 pixels. Thermal data has included an image sequence with more than a thousand images during the cooling period. The acquisition setup has been arranged to get images from the entire surface to ease the registration step. Figure 2 shows the thermograms in various orders after heating. As can be seen in the thermograms, the defect shape is altering according to cooling time. Early images have defect clues that seem more solid and sharp; however, later images look blurred and shady. The basis behind this imaging method is having discontinuities caused by the defect, which makes the heat transmission slower over the voids generated by the defect rather than the sound area. Thus, the thermal difference is able to display the defective regions. Although it has a wide range of application possibilities thanks to rapid and contactless nature, pulsed thermograpy is strongly affected by reflections from the environment, emissivity variations and nonuniform heating [12, 13].

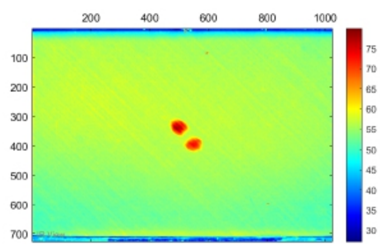

(a) First image after flash heating

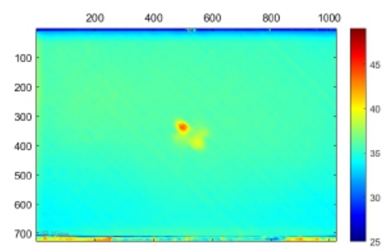

(b) Twenty-fifth image of sequence

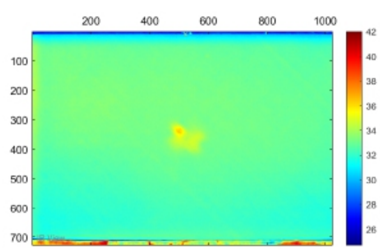

(c) Fourtieth image of sequence

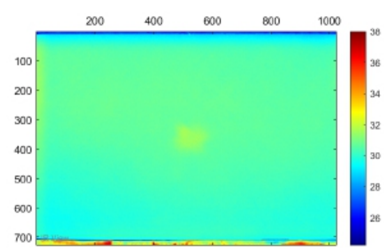

(d) Seventy-fifth image of sequence

Fig. 2 Raw thermograms in different orders to indicate the defect at various stages of cooling period

C. Phased array ultrasonic inspection

Ultrasonic inspection of these composite samples was performed by Sonatest Veo+ equipment and a 10 MHz phased array probe, including 64 element transducer with an appropriate wedge for ultrasonic wave transfer to the sample. The higher frequency probe provides better axial resolution through the thickness with the lower Signal-to-Noise ratio (SNR) due to the blind zone effect of the surface than the lower frequency probe [14]. The probe was moved on the surface of the sample, using sprayed water as a coupling mechanism, and an encoder followed the probe to measure the scanning distance. The PA ultrasonic data includes A-scan, cross-sectional form B-scan images and top-view C-scan images with depth information. Figure 3 presents these concepts for an 8 Joule-impacted sample to investigate ultrasonic signals that is originated from defect-free (non-defective) and defective regions. It should be noted that the PA scanning covered the full area (dimension) of the coupon (sample) to make it easier to align different source images.

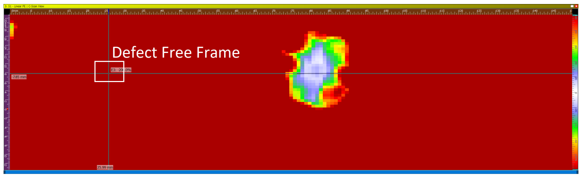

(a) Representative C-scan

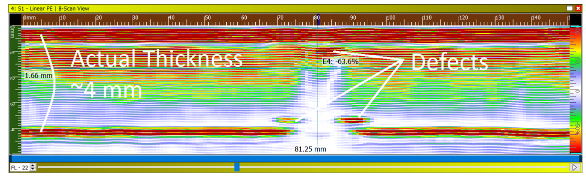

(b) Crass-sectional B-scan

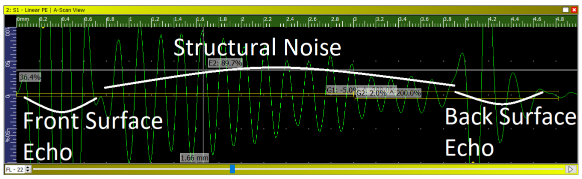

(c) A-scan signal form from a defect free frame

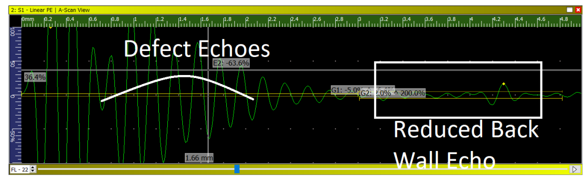

(d) A-scan from a defected frame

Fig. 3 A snapshot of raw defect detection on PA ultrasonic equipment for 8J impacted composite coupons

D. Pre-processing and fusion of images

An important step for efficient data fusion application is that of pre-processing. It will ensure that input data is fit for the fusion structure and utilisation of the fusion algorithm, as well as eliminate any noise or inconsistencies that may be present. As an example, in remote sensing data fusion applications the data pre-processing normally involves image registration, normalization, and filtering to ensure that the images are aligned and with consistent characteristics. Pre-processing may also involve feature extraction to reduce the dimensionality of the data and to identify the most relevant features for fusion. Inappropriate data pre-procesing tends to impact fusion outcomes, leading to inaccurate or unreliable results [15, 16].

To initiate the defect identification process, it is necessary to obtain images that differentiate between non-defective (sound) and defective regions. This is done using raw data from both imaging methods, i.e. from PA ultrasonic testing and from PT. As PAUT and PT data exhibit distinct characteristics, they must be processed separately to obtain images that provide meaningful information on defects and sound regions.

In the thermography inspection, a sequence of 1000 images is captured, depicting the cooling period of the material surface. The primary challenge is identifying the most representative image that can accurately display defects. To achieve this, an adaptive thresholding technique is employed, which adjusts the threshold level based on the sound regions present in each individual image of the sequence. Applying this technique enables easier determination of the size of any detected defects by analyzing the line profiles [17].

From the PA viewpoint, the obtained data comprises several signals for each frame of, per mm, dimension throughout the sample sizes. As it can be seen from the previous Figure, i.e. the A-scan signals snapshot, defect echoes need to be extracted by eliminating other echoes. This provides a location-based defect identification by applying smart thresholding method. Thresholding is carried out by trimming the peaks over the threshold, and finally, the amplitude values of defect signals were derived associated with their depth information. After thresholding operations and obtaining the binary defect images, the source images require an alignment process to provide accurate combination outcomes. Spatial referencing is a process used in image registration to align multiple images spatially in order to compare or merge these. This process involves identifying corresponding points or features in different images and then transforming the images to align them based on those points. Spatial referencing can be accomplished using a variety of techniques, including manual methods, feature-based methods, and intensity-based methods. In manual methods, corresponding points are identified manually by a user, whereas feature-based methods use automated algorithms to identify common features such as edges or corners. Intensity-based methods use the similarity of image intensity values to align images. Here, images have been aligned manually using the entire surface imaging and defect edges. Figure 4 schematizes the overall structure, including pre-processing, registration and fusion stages.

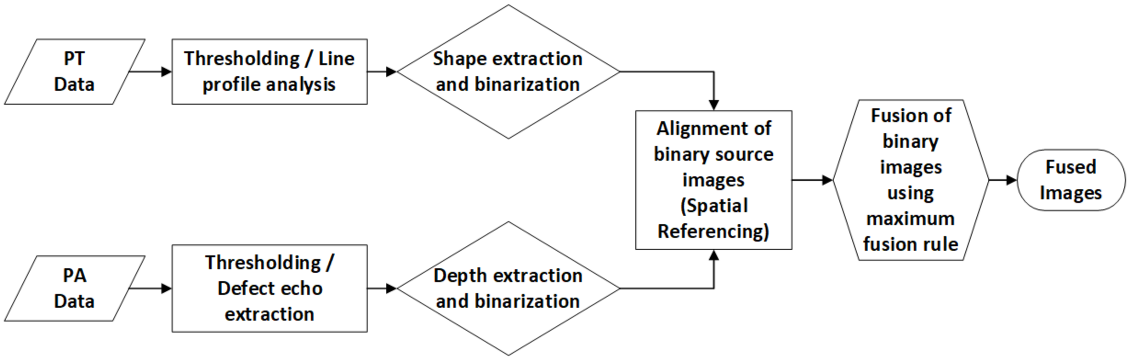

Fig. 4 Flow diagram of the proposed decision-level fusion approach

NDT fusion is a challenging subject given the dissimilar data acquisition environment of uni-modal inspections; there is some work on combining NDT techniques by fusion rules such as generic maximum, minimum or average merging by pixel-wise, principle component analysis (PCA) and wavelets, as well as AI-based approaches [10, 18–21]. In this study, we use the maximum combination rule, given in equations (1), as a simple yet effective synergistic approach to retrieve defect edges.

$$\tilde{F} = \max \bigcup_i F_i \tag{1}$$

Here, $\tilde{F}$ and F_i indicate the fused dataset and individual sources, respectively.

IV. Results and Discussion

Individual inspection images and binary forms extracted have been given in this section. Binarization of images is a widely used technique in image processing that involves converting grayscale or color images into binary images, which consist of only black and white pixels. This technique is useful in a variety of applications such as optical character recognition, image segmentation, and object detection. However, the choice of threshold value can have a significant impact on the accuracy and reliability of the binarization process. If the threshold value is set too low, the resulting binary image may include noise or other unwanted artefacts, whereas if it is set too high, important features or details may be lost. Therefore, choosing an appropriate threshold value is critical to achieving good results in binarization. Here, the adaptive threshold approach has been used to obtain precise detection results for defect detection.

Figure 5 shows PT inspection images in grey form with different levels of representativeness and their binarized states for 8J impacted specimen. As mentioned before, a significant step is to find the most representative image from the sequence of thousands of images. Here, the highest score of representation belongs to the image in the 31st row (Figure 5a). It should be stated that this image is not coming just after flash heating rather than the 10th image, which has evident pieces of defect clues but missing. Considering the three images in Figure 5b,5a and 5c, it can be noted claimed that the degree of representation first increased after the heating and then decreased with the increase in cooling. The 125th image looks almost indistinguishably cloudy. This is also evident in binary images. While the 31st image has an apparent defect shape which is better than 10th, the 125th image has highly poor defect clues.

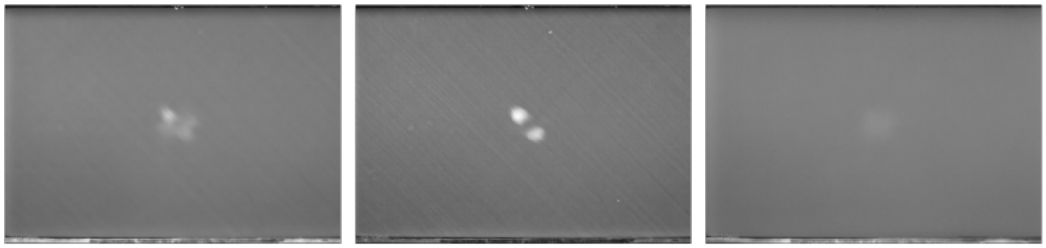

(a) Representative IRT image (31st) (b) Random weak representation of IRT (10th) (c) Random weaker representation of IRT (125th)

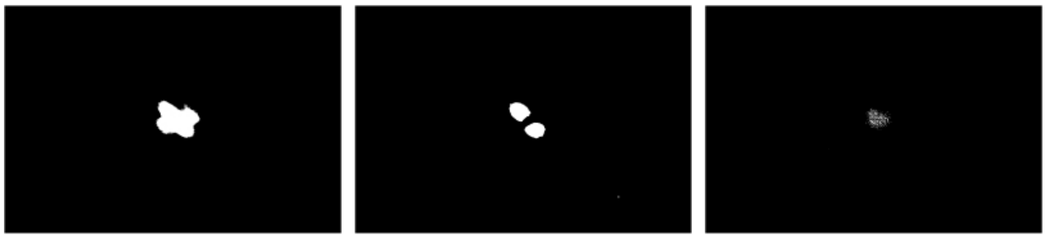

(d) Representative IRT image binary form (e) Weak representation binary form (f) Weaker representation binary form

Fig. 5 The best representative IRT image and two randomly selected images during cooling period and their binary forms

Figure 6 presents the depth information for three levels of impact damage, i.e. black color indicates regions close to the surface and white color indicates features deeper from surface. It should be emphasized here that damaged areas are seen not only in the area close to the surface but also deeper in the composite closer to back wall. It is noted that the defect sizes are increasing with the higher level of impact energy. Binary images of PA inspection emphasize the gradual increment in the defect size. Small distortion of the shape in binary images may require further investigation in selecting threshold values for related images.

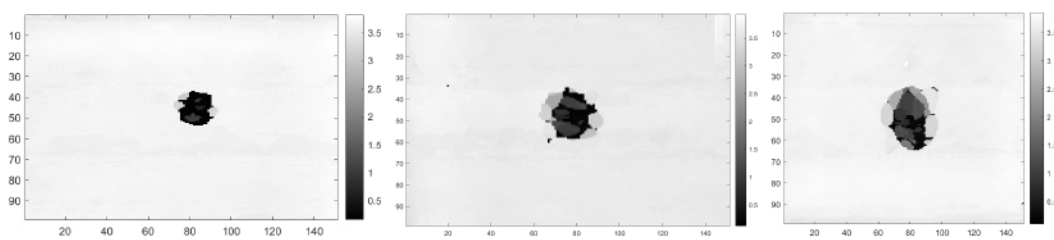

(a) 8J impact PA depth information (b) 12J impact PA depth information (c) 20J impact PA depth information

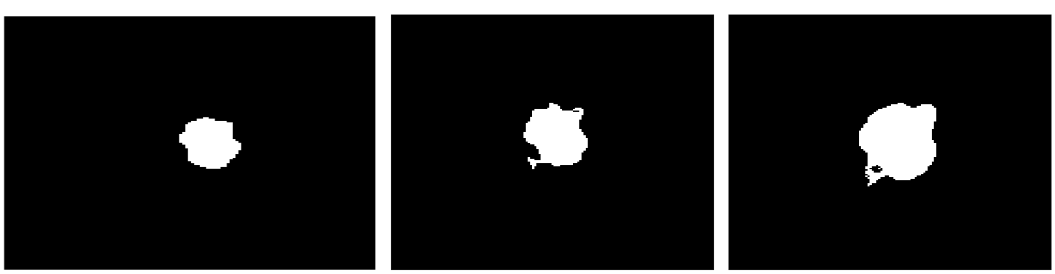

(d) 8J impact PA binary image (e) 12J impact PA binary image (f) 20J impact PA binary image

Fig. 6 Depth information of the samples extracted from PA inspection and binary forms after thresholding

Additionally, PA ultrasonic inspection is able to provide defect information layer by layer. Simply, Figure 7 has given defect marks for the first layer, second layer and up to middle layer of the composite structure. Images seem that the defect on the first layer is beginning outward from the inside; however, more concentrated at the edges in other layers.

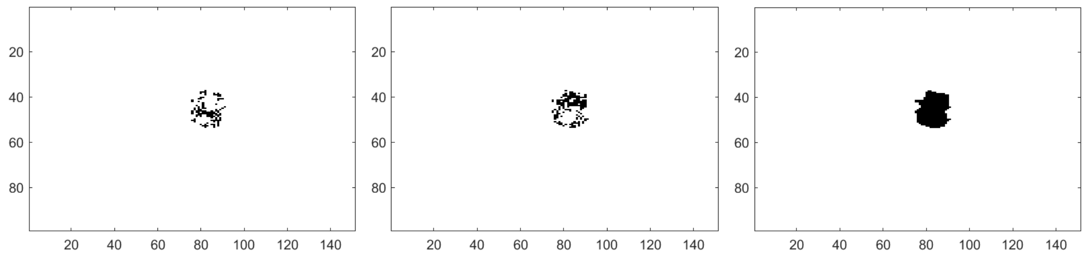

(a) Defect shape for the first layer (b) Defect shape between the first and second layer (c) Defect shape till midlayer

Fig. 7 Defect shapes for different depths, at first, second and up to middle layers

The fused image showcases the combined information and the resulting shape, and to improve the visualisation of the damage the images are binarized (see Figure 8). Fused images for all levels of impact energies have shown a more circular (round) and continuous form, unlike the sources. Inspection outputs obtained by both methods, although having minor morphological differences, provide consistent results that are mostly in agreement. The fused result combines information from both inspection approaches. It is clearly shown that the fusion approach can offer more efficient defect detection by combining the advantages of both inspection methods. This enhanced sizing of defect mechanisms can enable improved repair operations such as removing and patching [22].

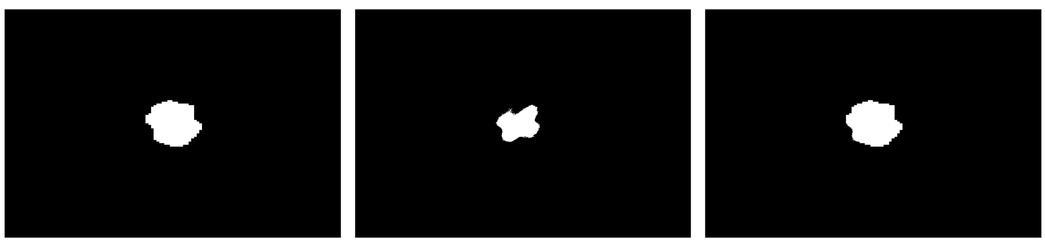

(a) 8J impact PA binary image (b) 8J impact IRT binary image (c) 8J impact fused image

(d) 12J impact PA binary image (e) 12J impact IRT binary image (f) 12J impact fused image

(g) 20J impact PA binary image (h) 20J impact IRT binary image (i) 20J impact fused image

Fig. 8 Processed source images and fused images for growing impact level using maximum rule

Table 1 Total defect sizes according to the impact levels and inspection results

Impact Level	Defect Region / cm^2		
	PA	**IRT**	**FUSED**
8J	3.60	2.05	3.67
12J	5.14	4.11	5.52
20J	8.52	6.24	9.19

Table 1 presents the calculated defect size. For all three cases, PA inspection outputs a larger defect area compared to IRT (PT). The fused images provide a more informative output by covering the wider area of the possible defect.

V. Conclusion and Further Steps

This study presented work on the effectiveness of fusing infrared thermography (IRT), specifically pulsed thermography (PT), and phased array ultrasonic testing (PA UT) inspection methods for the localization and characterization of impact defects in CFRP structures. By leveraging the strengths of both inspection techniques, the proposed fusion approach offers a more comprehensive and insightful evaluation of the defects. These findings can enable a better informed maintenance for the structural integrity of aircraft and hence contribute to improved Maintenance, Repair and Overhaul (MRO) activity.

Future research will explore and evaluate different fusion rules and structures against ground truth obtained from other inspection modalities. Work is also investigating the fusion of various types and energy levels of defects. The authors anticipate that these findings will stimulate further research interest in exploring NDT fusion strategies and support the development of more effective techniques for enhanced MRO.

References

[1] Braga, D. F., Tavares, S., Da Silva, L. F., Moreira, P., and De Castro, P. M., "Advanced design for lightweight structures: Review and prospects," Progress in Aerospace Sciences, Vol. 69, 2014, pp. 29–39.

[2] Towsyfyan, H., Biguri, A., Boardman, R., and Blumensath, T., "Successes and challenges in non-destructive testing of aircraft composite structures," Chinese Journal of Aeronautics, Vol. 33, No. 3, 2020, pp. 771–791.

[3] Senck, S., Scheerer, M., Revol, V., Dobes, K., Plank, B., and Kastner, J., "Non-destructive evaluation of defects in polymer matrix composites for aerospace applications using X-ray Talbot-Lau interferometry and micro CT," 58th AIAA/ASCE/AHS/ASC Structures, Structural Dynamics, and Materials Conference, 2017, p. 0355.

[4] Wang, B., Zhong, S., Lee, T.-L., Fancey, K. S., and Mi, J., "Non-destructive testing and evaluation of composite materials/structures: A state-of-the-art review," Advances in mechanical engineering, Vol. 12, No. 4, 2020, p. 1687814020913761.

[5] Mohammadkhani, R., Zanotti Fragonara, L., Padiyar M, J., Petrunin, I., Raposo, J., Tsourdos, A., and Gray, I., "Improving depth resolution of ultrasonic phased array imaging to inspect aerospace composite structures," Sensors, Vol. 20, No. 2, 2020, p. 559.

[6] Yuan, C., Xie, C., Li, L., Zhang, F., and Gubanski, S. M., "Ultrasonic phased array detection of internal defects in composite insulators," IEEE Transactions on Dielectrics and Electrical Insulation, Vol. 23, No. 1, 2016, pp. 525–531.

[7] Cullen, T. G., James, C. M., Ravichandran, R., Thompson, M., Moran, M., Ramesh, R., Morgan, R. G., and Nadesan, T., "Infrared thermography on a biconic model in Hypersonic expansion tube flows," AIAA Scitech 2021 Forum, 2021, p. 0873.

[8] Avdelidis, N., Gan, T.-H., Ibarra-Castanedo, C., and Maldague, X., "Infrared thermography as a nondestructive tool for materials characterisation and assessment," Thermosense: Thermal Infrared Applications XXXIII, Vol. 8013, SPIE, 2011, pp. 308–314.

[9] Maierhofer, C., Zacher, G., Kohl, C., and Wöstmann, J., "Evaluation of radar and complementary echo methods for NDT of concrete elements," Journal of Nondestructive Evaluation, Vol. 27, No. 1, 2008, pp. 47–57.

[10] Heideklang, R., and Shokouhi, P., "Fusion of multi-sensory NDT data for reliable detection of surface cracks: Signal-level vs. decision-level," AIP Conference Proceedings, Vol. 1706, AIP Publishing LLC, 2016, p. 180004.

[11] Shrestha, R., and Kim, W., "Non-destructive testing and evaluation of materials using active thermography and enhancement of signal to noise ratio through data fusion," Infrared Physics & Technology, Vol. 94, 2018, pp. 78–84.

[12] Benítez, H. D., Ibarra-Castanedo, C., Bendada, A., Maldague, X., Loaiza, H., and Caicedo, E., "Definition of a new thermal contrast and pulse correction for defect quantification in pulsed thermography," Infrared Physics & Technology, Vol. 51, No. 3, 2008, pp. 160–167. https://doi.org/https://doi.org/10.1016/j.infrared.2007.01.001, URL https://www.sciencedirect.com/science/article/pii/S135044950700014X.

[13] Tran, Q. H., Huh, J., Kang, C., Lee, B. Y., Kim, I.-T., and Ahn, J.-H., "Detectability of subsurface defects with different width-to-depth ratios in concrete structures using pulsed thermography," Journal of nondestructive evaluation, Vol. 37, 2018, pp. 1–11. https://doi.org/https://doi.org/10.1007/s10921-018-0489-x, URL https://link.springer.com/article/10.1007/s10921-018-0489-x.

[14] Padiyar M., J., Zanotti Fragonara, L., Petrunin, I., Raposo, J., Tsourdos, A., Gray, I., Farmaki, S., Exarchos, D., Matikas, T. E., and Dassios, K. G., "Fast, Accurate, and Reliable Detection of Damage in Aircraft Composites by Advanced Synergistic Infrared Thermography and Phased Array Techniques," Applied Sciences, Vol. 11, No. 6, 2021. https://doi.org/10.3390/app11062778, URL https://www.mdpi.com/2076-3417/11/6/2778.

[15] Choi, Y., Sharifahmadian, E., and Latifi, S., "Effect of pre-processing on satellite image fusion," The 17th CSI International Symposium on Computer Architecture & Digital Systems (CADS 2013), 2013, pp. 111–115. https://doi.org/10.1109/CADS.2013.6714246.

[16] Xiao, X., Xiao, Y., Zhang, Y., Qiu, J., Zhang, J., and Yildirim, T., "A fusion data preprocessing method and its application in complex industrial power consumption prediction," Mechatronics, Vol. 77, 2021, p. 102520. https://doi.org/https://doi.org/10.1016/j.mechatronics.2021.102520, URL https://www.sciencedirect.com/science/article/pii/S095741582100026X.

[17] Avdelidis, N., Hawtin, B., and Almond, D., "Transient thermography in the assessment of defects of aircraft composites," NDT & E International, Vol. 36, No. 6, 2003, pp. 433–439. https://doi.org/https://doi.org/10.1016/S0963-8695(03)00052-5, URL https://www.sciencedirect.com/science/article/pii/S0963869503000525.

[18] Zhou, Y., Yu, L., Zhi, C., Huang, C., Wang, S., Zhu, M., Ke, Z., Gao, Z., Zhang, Y., and Fu, S., "A Survey of Multi-Focus Image Fusion Methods," Applied Sciences, Vol. 12, No. 12, 2022, p. 6281.

[19] Wu, Y.-J., Shi, X.-Z., and Zhuang, T. G., "Fusion of wavelet packets and neural network in detection of composites," AIAA journal, Vol. 38, No. 6, 2000, pp. 1063–1069.

[20] Wei, Y., Ye, Y., He, H., Su, Z., Ding, L., and Zhang, D., "Multi-frequency Fused Lock-in Thermography in Detecting Defects at Different Depths," Journal of Nondestructive Evaluation, Vol. 41, No. 3, 2022, pp. 1–10.

[21] Hu, J., Zhang, H., Sfarra, S., Pivarčiová, E., Yao, Y., Duan, Y., Ibarra-Castanedo, C., Tian, G., and Maldague, X., "Autonomous dynamic line-scan continuous-wave terahertz non-destructive inspection system combined with unsupervised exposure fusion," NDT & E International, Vol. 132, 2022, p. 102705.

[22] Kostopoulos, V., Psarras, S., Loutas, T., Sotiriadis, G., Gray, I., Padiyar, M., Petrunin, I., Raposo, J., Fragonara, L. Z., Tzitzilonis, V., Dassios, K., Exarchos, D., Andrikopoulos, G., and Nikolakopoulos, G., "Autonomous Inspection and Repair of Aircraft Composite Structures," IFAC-PapersOnLine, Vol. 51, No. 30, 2018, pp. 554–557. https://doi.org/https://doi.org/10.1016/j.ifacol.2018.11.267, URL https://www.sciencedirect.com/science/article/pii/S2405896318329409, 18th IFAC Conference on Technology, Culture and International Stability TECIS 2018.

2023-06-08

Fusion insights from ultrasonic and thermographic inspections for impact damage analysis

Torbali, M. Ebubekir

AIAA

Torbali ME, Alhammad M, Zolotas A, et al., (2023) Fusion insights from ultrasonic and thermographic inspections for impact damage analysis. In: 2023 AIAA Aviation and Aeronautics Forum and Exposition (AIAA AVIATION Forum), 12-16 June 2023, San Diego, CA

https://doi.org/10.2514/6.2023-3867